

J-CAMD 272

## Prediction of the binding site of 1-benzyl-4-[(5,6-dimethoxy-1-indanon-2-yl)methyl]piperidine in acetylcholinesterase by docking studies with the SYSDOC program

Yuan-Ping Pang\* and Alan P. Kozikowski\*\*

*Neurochemistry Research, Mayo Foundation for Medical Education and Research, 4500 San Pablo Road,  
Jacksonville, FL 32224, U.S.A.*

Received 13 April 1994

Accepted 12 August 1994

*Key words:* Molecular recognition; E2020; Acetylcholinesterase inhibitors; Alzheimer's disease

---

### SUMMARY

In the preceding paper we reported on a docking study with the SYSDOC program for predicting the binding sites of huperzine A in acetylcholinesterase (AChE) [Pang, Y.-P. and Kozikowski, A.P., *J. Comput.-Aided Mol. Design*, 8 (1994) 669]. Here we present a prediction of the binding sites of 1-benzyl-4-[(5,6-dimethoxy-1-indanon-2-yl)methyl]piperidine (E2020) in AChE by the same method. E2020 is one of the most potent and selective reversible inhibitors of AChE, and this molecule has puzzled researchers, partly due to its flexible structure, in understanding how it binds to AChE. Based on the results of docking 1320 different conformers of E2020 into 69 different conformers of AChE and on the pharmacological data reported for E2020 and its analogs, we predict that both the *R*- and the *S*-isomer of E2020 span the whole binding cavity of AChE, with the ammonium group interacting mainly with Trp<sup>84</sup>, Phe<sup>330</sup> and Asp<sup>72</sup>, the phenyl group interacting mainly with Trp<sup>84</sup> and Phe<sup>330</sup>, and the indanone moiety interacting mainly with Tyr<sup>70</sup> and Trp<sup>279</sup>. The topography of the calculated E2020 binding sites provides insights into understanding the high potency of E2020 in the inhibition of AChE and provides hints as to possible structural modifications for identifying improved AChE inhibitors as potential therapeutics for the palliative treatment of Alzheimer's disease.

---

### INTRODUCTION

Among the different classes of acetylcholinesterase (AChE) inhibitors reported to date [1–6], 1-benzyl-4-[(5,6-dimethoxy-1-indanon-2-yl)methyl]piperidine (E2020, Fig. 1) has attracted much

---

\*To whom correspondence should be addressed.

\*\*Present address: Trophix Pharmaceuticals, Inc., 89 Headquarters Plaza, North Tower, 14th Floor, Morristown, NJ 07960, U.S.A.

attention as a possible therapeutic agent in the palliative treatment of mild or moderate forms of Alzheimer's disease. E2020 is readily synthesized and has higher potency in inhibiting AChE, higher selectivity for AChE versus butyrylcholinesterase, and longer duration of action in comparison with physostigmine and tacrine [5]. In terms of size and structural flexibility, it resembles the decamethonium cation that is reported to bind to the cavity of AChE (the gorge) by spanning the whole gorge, with its two ammonium groups interacting with Trp<sup>84</sup> at the bottom and Trp<sup>279</sup> at the opening of the gorge [7]. However, unlike the decamethonium cation, E2020 possesses only one ammonium group, which may interact with either Trp<sup>84</sup> or Trp<sup>279</sup>. In addition, unlike other structural types of AChE inhibitors, E2020 possesses two aromatic functional groups and exhibits no stereoselectivity (both the *R*- and the *S*-isomer have been reported to be equally active) [8]. These complicated features of E2020 have puzzled researchers in understanding how the molecule binds to AChE, thereby inhibiting the enzyme. Extensive conformational and QSAR studies on E2020 and its analogs have been carried out in attempts to postulate the active conformation of E2020. These modeling efforts were reported before the crystal structure of AChE was published in 1991 [8–10], and no detailed information as to how this molecule binds to the gorge has become available since then [11]. The lack of such information is partly due to the conformational flexibility of E2020. The E2020 molecule possesses six rotatable bonds, one flexible six-membered ring and one freely invertible nitrogen atom. As discussed in the preceding paper [12], to permit the guest and the host to change their conformations upon binding, different conformations with relatively low potential energy must be taken into account in the docking studies. Therefore, a rigorous docking study of E2020 requires a tremendous amount of computing time.

In this article, we report our docking study of E2020 and predict its binding sites in AChE. The topography of the calculated binding sites should provide insights into the potency of E2020 in inhibiting AChE and provide a basis for structural modifications aimed at finding better AChE inhibitors as potential therapeutics for the palliative treatment of Alzheimer's disease.

## DOCKING STRATEGY

From a structural point of view, a conformational change at the two methoxyl groups of E2020 does not change the overall backbone conformation (steric and electrostatic fields) of E2020. From a pharmacological point of view, removing these methoxyl groups only gradually reduces the inhibition of AChE [5]. We therefore decided to dock first a pre-E2020 molecule,

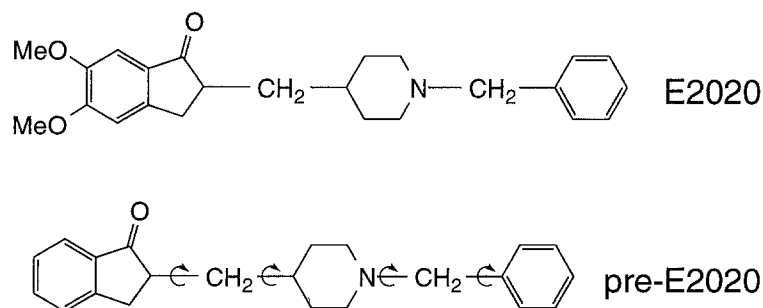


Fig. 1. Structures of E2020 and pre-E2020 with the defined rotatable bonds.

possessing no methoxyl groups (Fig. 1), in order to eliminate conformers that do not fit into the topography of the gorge, then to derivatize all suitable conformers of pre-E2020 by adding the two missing methoxyl groups with different sets of torsional angles, and lastly to dock all resulting conformers of E2020. In this way, we efficiently reduce a large conformational search space for E2020 (theoretically 2.9 million conformations for six rotatable bonds at a 30° torsional increment) to a much smaller conformational search space for pre-E2020 (theoretically 20 000 conformations for four rotatable bonds at a 30° torsional increment), and dock only a relatively small number of preselected conformers of E2020. Since both enantiomers of E2020 are active, both compounds must be considered in the docking studies.

## CONFORMATIONAL SEARCH

In the conformational search on both enantiomers of pre-E2020 employing the SysSearch program [13], four rotatable bonds were defined as depicted in Fig. 1, the torsional increment was set to 30°, the van der Waals factor to 0.8, and the potential energy thresholds for the structures that were subjected to further energy minimization and docking to 50 and 40 kcal/mol, respectively. The amino group of pre-E2020 was treated as an ammonium cation. The piperidine ring was confined to its two chair conformations, with each of its appendages at either an axial or equatorial position, which permits the inversion of the nitrogen atom prior to its protonation. Two conformers were judged different if one of the above-defined torsional angles differed by more than 30°. The SysSearch program generated 120 different conformers of (*R*)-pre-E2020 and 104 different conformers of (*S*)-pre-E2020. In the conformational search on 5,6-dimethoxy-1-indanone, that is a substructure of E2020, the two single bonds between the oxygen atom and the aromatic ring were defined as rotatable bonds, the rotational increment was set to 30°, the van der Waals factor to 0.8, and the potential energy thresholds for the structures that were subjected to further energy minimization and docking to 50 and 40 kcal/mol, respectively. Twenty-two different conformers of 5,6-dimethoxy-1-indanone were obtained, and the corresponding sets of torsional angles were later used for derivatizing pre-E2020.

## DOCKING STUDIES

We docked 120 different conformers of (*R*)-pre-E2020 and 104 different conformers of (*S*)-pre-E2020, employing the SYSDOC program as described in the preceding paper, into a box (17.3 × 17.4 × 19.7 Å), which encompasses the space confined by the 14 aromatic residues on the surface of the gorge in 69 different conformers of *Torpedo* AChE. The conformers of AChE used for docking were selected from an ensemble of conformers of *Torpedo* AChE obtained from the dynamics simulations, in which the entire protein was allowed to move at 300 K in vacuo for 40 ps as described in the preceding paper. The docking of all different conformers of pre-E2020 was performed by rotating pre-E2020 at 20° arc increments around the x, y and z axes and translating it at 1.0 Å increments along the x, y and z axes in the above-mentioned box; the docking was not subjected to fine-tuning. The pre-E2020 docking revealed that 36 different conformers of the *R*-isomer and 24 different conformers of the *S*-isomer possess a suitable backbone conformation to fit into the gorge of AChE. Next, each of these selected conformers was derivatized as indicated above by adding the missing methoxyl groups in 22 different conformations. Finally, the

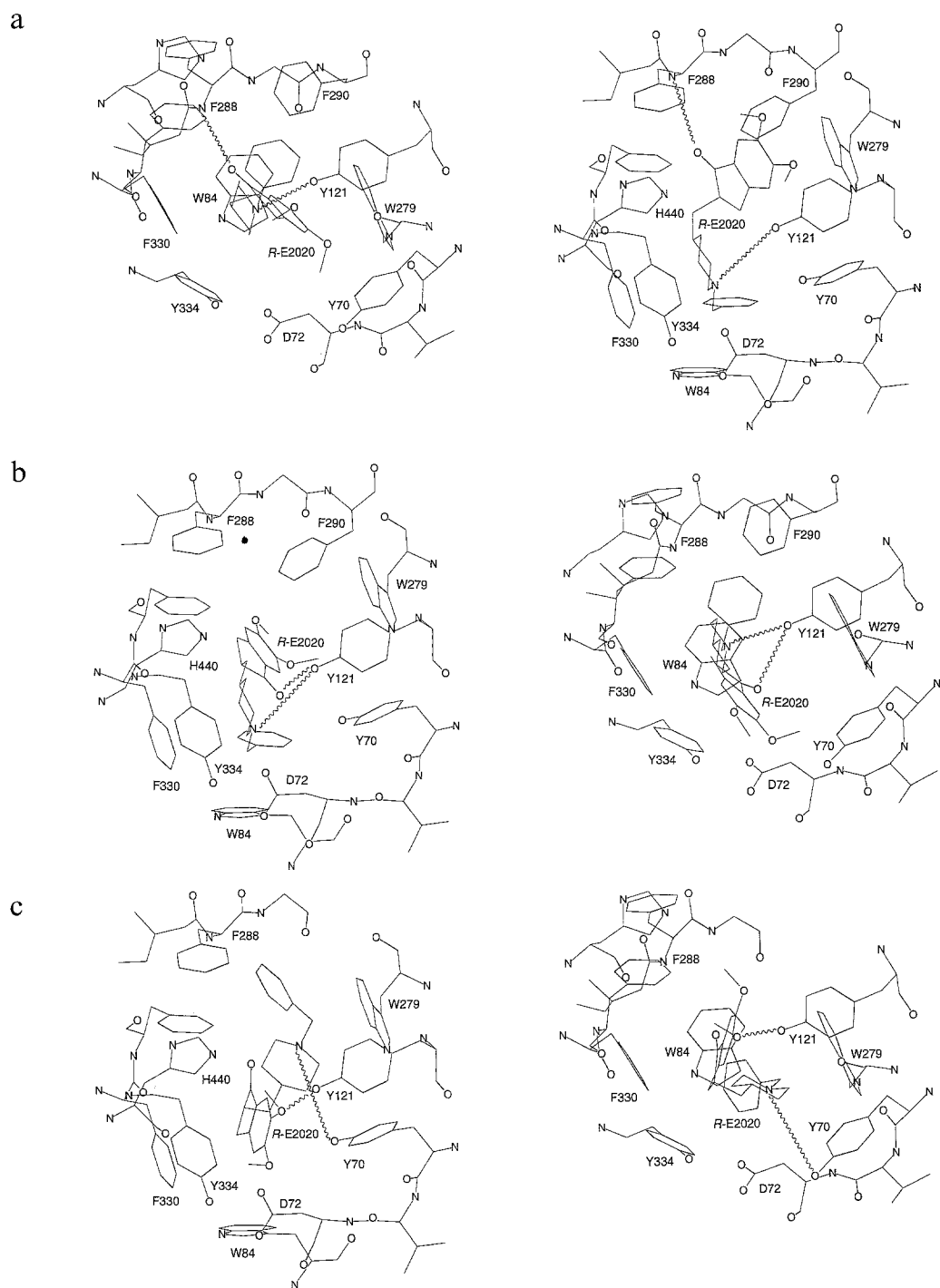
resulting 792 different conformers of (*R*)-E2020 and 528 different conformers of (*S*)-E2020 were docked into the 69 conformers of AChE with the same docking protocol as used in docking pre-E2020, and this result was fine-tuned at 5° arc increment in a range of 30° of arc and at 0.2 Å increment in a range of 1.2 Å. The docking studies, together with the conformational search, took about two weeks of CPU time on two IBM RS/6000, one SGI R4000 and one DEC alpha 3000 computer.

### BINDING SITES OF (*R*)-E2020

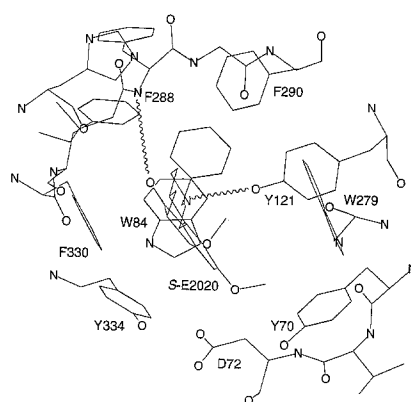
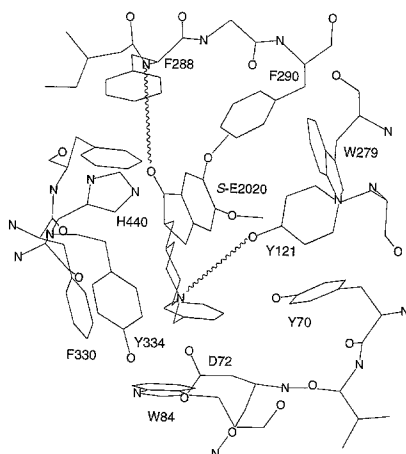
The docking studies reveal that (*R*)-E2020 possesses three overlapping binding sites, and that at each site it spans the whole gorge. Sites I and II are more favorable than site III, as demonstrated by the binding energies of sites I, II and III: -65.1, -60.6 and -55.8 kcal/mol, respectively. These binding energies, relative to AChE and E2020 in their free state, were calculated employing the CHARMM program with its all-atom force field and distance-dependent dielectric constant. This was done by subtracting the sum of the potential energies of the separated AChE and E2020, whose conformations are identical to those in the E2020-AChE complex, from the potential energy of the complex (the differences of these energies are identical to those calculated by SYSDOC with TRIPOS or the all-atom CHARMM force field). At site I (Fig. 2a; the coordinates of the SYSDOC-generated complexes in Fig. 2 will be deposited in the Brookhaven Protein Data Bank [14]), the ammonium group interacts with the aromatic groups of Trp<sup>84</sup>, Phe<sup>330</sup> and Tyr<sup>334</sup> as well as the carboxyl group of Asp<sup>72</sup>; the phenyl group interacts with the aromatic groups of Trp<sup>84</sup> and Phe<sup>330</sup>; the indanone moiety interacts with the aromatic groups of Tyr<sup>70</sup>, Tyr<sup>121</sup>, Trp<sup>279</sup> and Phe<sup>290</sup>; the carbonyl oxygen atom forms a hydrogen bond with the amide hydrogen atom of Phe<sup>288</sup>; and the proton at the piperidine nitrogen forms a hydrogen bond with the hydroxyl oxygen atom of Tyr<sup>121</sup>. At site II (Fig. 2b), the ammonium group interacts with the aromatic groups of Trp<sup>84</sup>, Phe<sup>330</sup> and Tyr<sup>334</sup> as well as the carboxyl group of Asp<sup>72</sup>; the phenyl group interacts with the aromatic groups of Trp<sup>84</sup> and His<sup>440</sup>; the indanone moiety interacts with the aromatic groups of Tyr<sup>70</sup>, Tyr<sup>334</sup> and Trp<sup>279</sup>; the carbonyl oxygen atom forms a hydrogen bond with the hydroxyl hydrogen atom of Tyr<sup>121</sup>; and the proton at the piperidine nitrogen forms a hydrogen bond with the hydroxyl oxygen atom of Tyr<sup>121</sup>. At site III (Fig. 2c), the ammonium group interacts with the aromatic groups of Tyr<sup>70</sup>, Tyr<sup>121</sup> and Trp<sup>279</sup>; the phenyl group interacts with the aromatic group of Trp<sup>279</sup>; the indanone moiety interacts with the aromatic groups of Trp<sup>84</sup>, Phe<sup>330</sup> and Tyr<sup>334</sup>; the methoxyl oxygen atom at the 6-position of the indanone forms a hydrogen bond with the hydroxyl hydrogen atom of Tyr<sup>121</sup>; and the proton at the piperidine nitrogen forms a hydrogen bond with the hydroxyl oxygen atom of Tyr<sup>70</sup>. As is apparent from Figs. 2a and b, site I is different from site II only in that the hydrogen bond donor for the carbonyl oxygen atom of E2020 is the amide hydrogen atom of Phe<sup>288</sup> at site I and the hydroxyl hydrogen atom of Tyr<sup>121</sup> at site II. The two methoxyl groups of (*R*)-E2020 are exposed to the solvent at sites I and II.

### BINDING SITES OF (*S*)-E2020

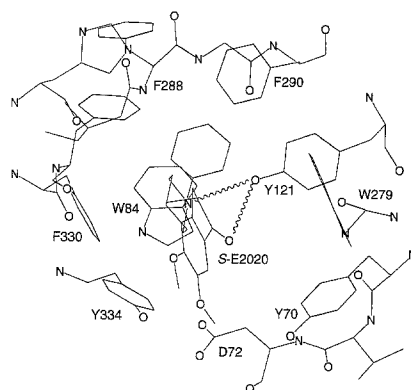
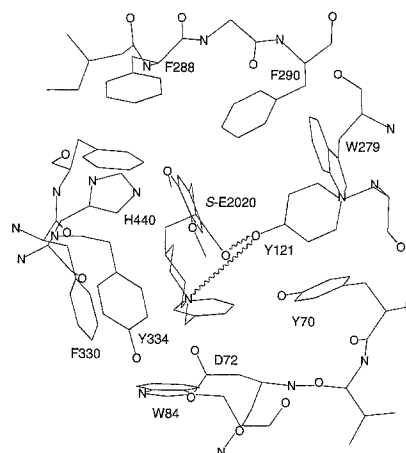
Similar to *R*-E2020, (*S*)-E2020 possesses three overlapping binding sites, two of which (sites I and II, whose binding energies are -63.2 and -64.5 kcal/mol, respectively) are more favorable



d



e



f

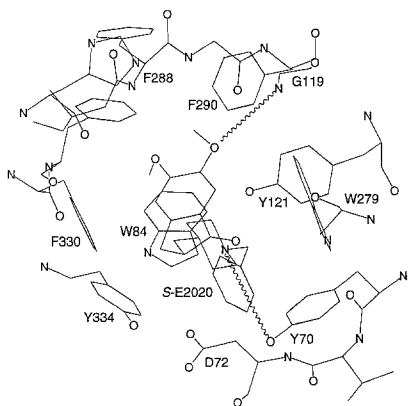
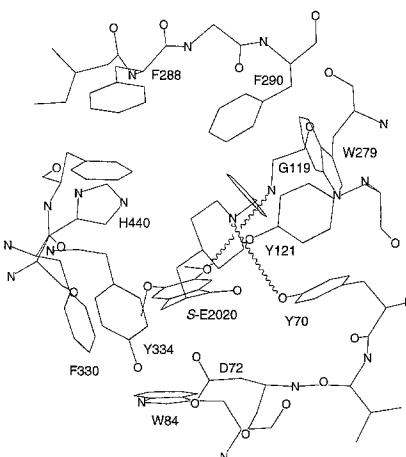


Fig. 2. (continued).

than the third (site III,  $-56.0$  kcal/mol), and at each site it spans the whole gorge. At site I (Fig. 2d), the ammonium group interacts with the aromatic groups of Trp<sup>84</sup> and Phe<sup>330</sup> as well as the carboxyl group of Asp<sup>72</sup>; the phenyl group interacts with the aromatic groups of Trp<sup>84</sup>, Phe<sup>330</sup> and His<sup>440</sup>; the indanone moiety interacts with the aromatic groups of Tyr<sup>70</sup>, Tyr<sup>121</sup>, Tyr<sup>334</sup> and Trp<sup>279</sup>; the carbonyl oxygen atom forms a hydrogen bond with the amide hydrogen atom of Phe<sup>288</sup>; and the proton at the piperidine nitrogen forms a hydrogen bond with the hydroxyl oxygen atom of Tyr<sup>121</sup>. At site II (Fig. 2e), the ammonium group interacts with the aromatic groups of Trp<sup>84</sup>, Phe<sup>330</sup> and Tyr<sup>334</sup> as well as the carboxyl group of Asp<sup>72</sup>; the phenyl group interacts with the aromatic groups of Trp<sup>84</sup>, Phe<sup>330</sup>, Tyr<sup>334</sup> and His<sup>440</sup>; the indanone moiety interacts with the aromatic groups of Tyr<sup>70</sup>, Tyr<sup>334</sup> and Trp<sup>279</sup>; the carbonyl oxygen atom forms a hydrogen bond with the hydroxyl hydrogen atom of Tyr<sup>121</sup>; and the proton at the piperidine nitrogen forms a hydrogen bond with the hydroxyl oxygen atom of Tyr<sup>121</sup>. At site III (Fig. 2f), the ammonium group interacts with the aromatic groups of Tyr<sup>70</sup> and Trp<sup>279</sup>; the phenyl group interacts with the aromatic groups of Tyr<sup>70</sup> and Trp<sup>279</sup>; the indanone moiety interacts with the aromatic groups of Trp<sup>84</sup>, Phe<sup>330</sup>, Tyr<sup>334</sup> and His<sup>440</sup>; the methoxyl oxygen atom at the 6-position of the indanone forms a hydrogen bond with the amide hydrogen atom of Gly<sup>119</sup>; and the proton at the piperidine nitrogen forms a hydrogen bond with the hydroxyl oxygen atom of Tyr<sup>70</sup>. Similar to *R*-E2020, site I is different from site II only in that the hydrogen bond donor for the carbonyl oxygen atom of E2020 is the amide hydrogen atom of Phe<sup>288</sup> at site I and the hydroxyl hydrogen atom of Tyr<sup>121</sup> at site II. The two methoxyl groups of the *S*-isomer are exposed to the solvent at sites I and II.

## EXPERIMENTAL SUPPORT

The predicted hydrogen bond to the carbonyl oxygen atom in E2020 for both enantiomers is supported by the weak inhibition of analog **1** [5] (see data in Fig. 3). Although the optical purity of compound **1** was not reported, the 53-fold difference in AChE inhibition between E2020 and **1** does not likely result from the presence of the improper diastereomer of compound **1**. The weak inhibition is due to the reduction of the carbonyl group of E2020 to an alcohol as in **1**, which moves the carbonyl group away from the hydrogen bond donor. The predicted hydrogen bond originating from the proton at the piperidine nitrogen of E2020 is also supported by the weak inhibitory effect of analog **2** [5], whose nitrogen atom has been displaced from the preferred hydrogen bond donor site (Fig. 3). The predicted  $\pi$ - $\pi$  interaction of the indanone moiety and the phenyl group of E2020 with the aromatic gorge is supported by the reduced AChE inhibitory activity shown by analogs **3** and **4** [5]. In analog **3**, the  $\pi$  electron density is reduced in the indanone portion due to the absence of the two methoxyl groups, while in structure **4**, the  $\pi$  electrons of the phenyl group are missing altogether.

## DISCUSSION

As stated in the preceding paper, the direct interaction of the guest with the solvent molecules is ignored in the current version of SYSDOC. The exposure of the two methoxyl oxygen atoms of E2020 to the solvent (water) molecules at sites I and II provides the possibility for water molecules to bridge the interactions between E2020 and the gorge by forming concurrent hydro-

gen bonds with the methoxyl oxygen atoms of E2020 and the polar hydrogen atoms of the gorge. Consequently, the binding energy contributed by solvation effects is not included in the energy calculation of SYSDOC, which results in an underestimation of the binding energy at sites I and II. In general, the neglect of the direct interaction of the guest with solvent molecules will underestimate the binding energy at such sites where the hydrogen bond acceptors of the guest are exposed to the solvent. However, this limitation can be overcome by free energy perturbation studies through dynamics simulations with the SYSDOC-generated complex in solvent, or by human intuition together with structure–activity relationship studies of a series of analogs.

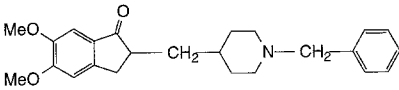
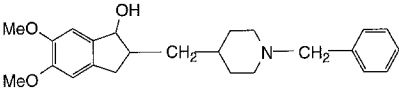
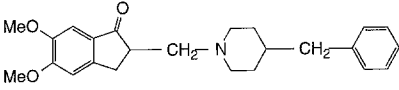
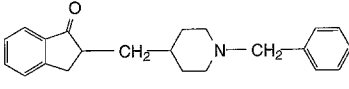
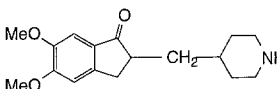
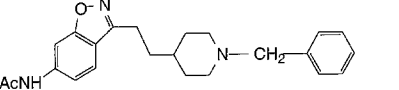
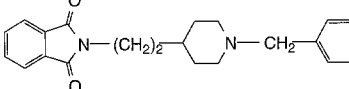
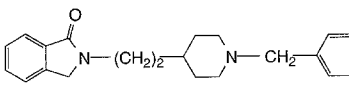
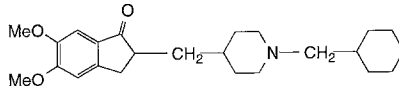
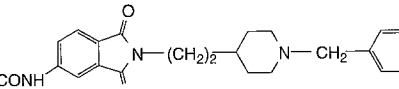
	AChE Inhibition IC <sub>50</sub> (nM)	
	<b>±E2020</b>	5.7 ± 0.2
	<b>1</b>	300
	<b>2</b>	480
	<b>3</b>	150
	<b>4</b>	5400
	<b>5</b>	3.0
	<b>6</b>	30
	<b>7</b>	98
	<b>8</b>	8.9
	<b>9</b>	1.2

Fig. 3. E2020 analogs with their IC<sub>50</sub> values of AChE inhibition.



Therefore, based on the above-described binding energies of sites I, II and III for both enantiomers of E2020 and the structure–activity relationship studies of all compounds listed in Fig. 3, we predict that sites I and II are the binding sites in AChE for both enantiomers of E2020. Although the conformation of (*R*)-E2020 at site III is identical (by visual inspection) to Hopfinger's postulated active conformation of (*R*)-E2020 [8], we currently believe that site III is an unlikely, but not impossible, candidate as the binding site in AChE for E2020. It should be noted that the objective of the docking studies is to search for *likely* binding sites, rather than to determine the actual binding sites, and that the true advantage of the docking studies stems from the ability to eliminate *billions* of impossible binding sites. In support of our results, researchers at Pfizer have identified a binding site in AChE for an E2020 analog (**5**, Fig. 3) whose binding motif is similar to that provided by sites I and II. The Pfizer group employed extended dynamics simulations in water [15]. At the site identified by the Pfizer group, the phenyl group of **5** interacts with Trp<sup>84</sup>, the ammonium group interacts with the carboxyl group of Asp<sup>72</sup>, and the oxygen atom forms a hydrogen bond with the amide hydrogen atom of Phe<sup>288</sup>.

Paralleling the complications arising from the possibility of multiple binding sites for huperzine A in the bottom of the gorge, as described in the preceding paper, we cannot specify which site, I or II, is preferred for E2020. Three possibilities are therefore conceivable for this molecule:

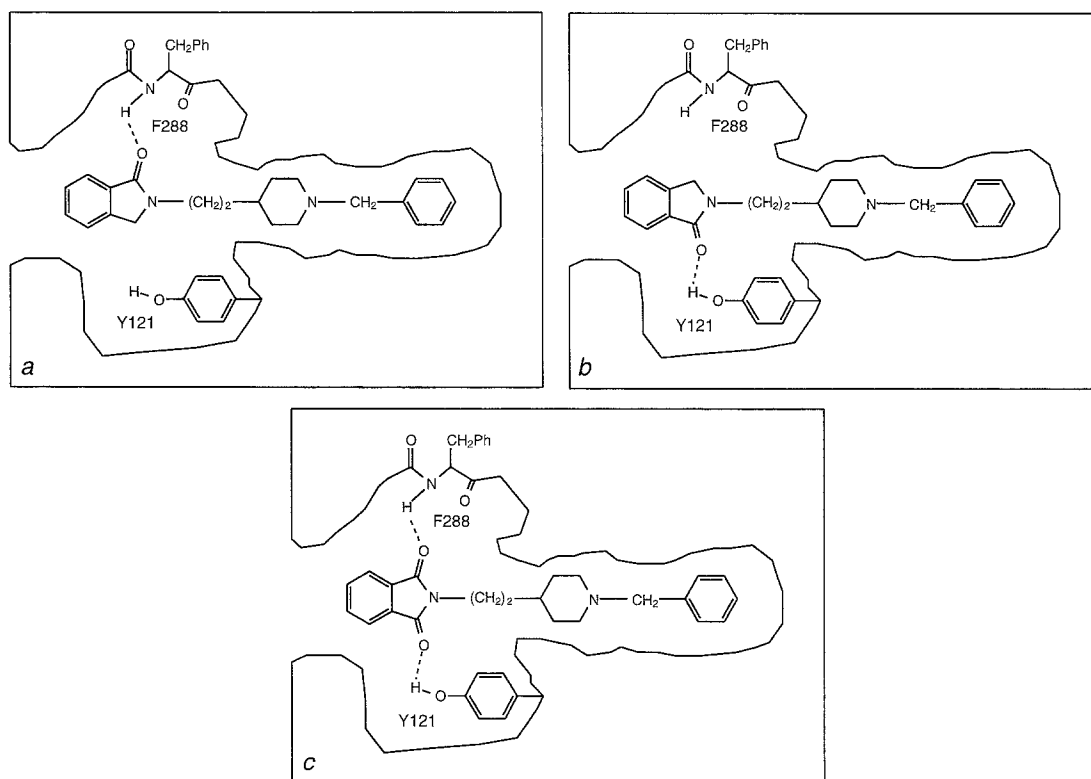


Fig. 4. Topography of the binding site of analog **6**, emphasizing the possibilities for hydrogen bond formation at sites I and II (---: hydrogen bond).

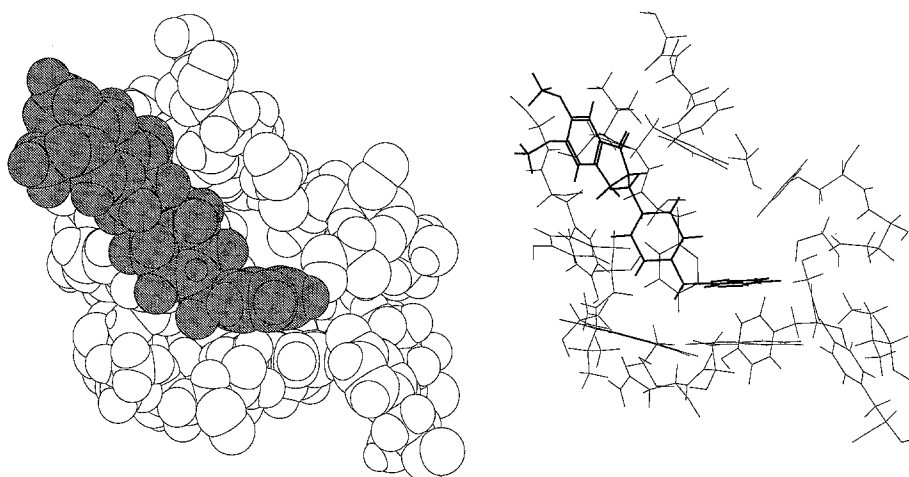


Fig. 5. Left: the spacefilling representation (shaded: (*R*)-E2020; white: the gorge) and right: the wire frame representation (bold: (*R*)-E2020; thin: the gorge) of the gorge bound with (*R*)-E2020.

(i) that E2020 may bind to only one site and the other one is an artifact; (ii) that it binds to one site under some conditions and to the other site under other conditions; and (iii) that it switches among these two sites. The first possibility is, however, rendered unlikely by the fact that analog **6** [16] is more potent in the inhibition of AChE than analog **7** [16]. The increased inhibitory potency shown by **6** is compatible with the notion that **6** forms one more hydrogen bond to AChE (Fig. 4c) than does **7** (Figs. 4a and b), i.e., **6** simultaneously forms two relatively weak hydrogen bonds or one strong and one weak hydrogen bond with the amide hydrogen atom of Phe<sup>288</sup>, a hydrogen bond donor located at site I (Fig. 4a), and the hydroxyl hydrogen atom of Tyr<sup>121</sup> located at site II (Fig. 4b). The strength of a hydrogen bond is estimated by the distance between the hydrogen bond donor and acceptor. The relatively small increase in AChE inhibition caused by the introduced weak hydrogen bond between **6** and AChE is also due to the solvation energy change of **6**, caused by the introduced carbonyl group and the possible loss of entropy for **6** relative to **7** at the binding site. Thus, by inference both sites I and II may be available to E2020. Further experimental investigations into the dynamics of binding of E2020 to AChE will be required to sort out the last two possibilities.

It is conceivable from the description of the binding sites of E2020 that the compound's high potency in AChE inhibition is partly due to the aromatic–aromatic interactions [17,18] in the opening of the gorge and at the bottom of the gorge. In contradiction to this idea, analog **8** [5], in which the phenyl group has been replaced by a nonaromatic cyclohexyl group, is almost as active as E2020. Tentatively, this result can be explained by assuming that the attractive London dispersion forces between the gorge and the cyclohexyl group occupying the unfilled space between the phenyl group of E2020 and the gorge (Fig. 5) compensate for the loss of the aromatic–aromatic interactions at the bottom of the gorge. The retention of inhibitory activity in analog **8** suggests that structural modifications to the phenyl portion of E2020 or analog **9** [16] (Fig. 3), by either increasing size and/or altering the  $\pi$  electron density, might further increase inhibitory potency.

## ACKNOWLEDGEMENTS

We thank Professor Joel L. Sussman of the Weizmann Institute of Science in Israel for providing the crystal structures of inhibitor-bound AChE, Professor Martin Karplus of Harvard University and the reviewers for their comments and Mr. Fred Pishotta of the Mayo Foundation for support of computing resources. Support by the Mayo Foundation, NIA (A.P.K.) and IBM (Y.-P.P.) is gratefully acknowledged.

## REFERENCES

- 1 Han, S.Y., Sweeney, J.E., Bachman, E.S., Schweiger, E.J., Forloni, G., Coyle, J.T., Davis, B.M. and Joullie, M.M., *Eur. J. Med. Chem.*, 27 (1992) 673.
- 2 Pomponi, M., Giardina, B., Gatta, F. and Marta, M., *Med. Chem. Res.*, 2 (1992) 306.
- 3 Wilson, I.B. and Quan, C., *Arch. Biochem. Biophys.*, 73 (1958) 131.
- 4 Brimijoin, S., Hammond, P. and Rakonczay, Z., *J. Neurochem.*, 49 (1987) 555.
- 5 Sugimoto, H., Iimura, Y., Yamanishi, Y. and Yamatsu, K., *Bioorg. Med. Chem. Lett.*, 8 (1992) 871.
- 6 Kozikowski, A.P., Miller, C.P., Yamada, F., Pang, Y.-P., Miller, J.H., McKinney, M. and Ball, R.G., *J. Med. Chem.*, 34 (1991) 3399.
- 7 Harel, M., Schalk, I., Ehretsabatier, L., Bouet, F., Goeldner, M., Hirth, C., Axelsen, P.H., Silman, I. and Sussman, J.L., *Proc. Natl. Acad. Sci. USA*, 90 (1993) 9031.
- 8 Cardozo, M.G., Kawai, T., Iimura, Y., Sugimoto, H., Yamanishi, Y. and Hopfinger, A.J., *J. Med. Chem.*, 35 (1992) 590.
- 9 Cardozo, M.G., Iimura, Y., Sugimoto, H., Yamanishi, Y. and Hopfinger, A.J., *J. Med. Chem.*, 35 (1992) 584.
- 10 Sussman, J.L., Harel, M., Frolow, F., Oefner, C., Goldman, A., Toker, L. and Silman, I., *Science*, 253 (1991) 872.
- 11 Gubernator, K., Ammann, H.J., Broger, C., Bur, D., Doran, D.M., Berber, P.R., Muller, K. and Schaumann, T.M., In Wermuth, C.G. (Ed.) *Trends in QSAR and Molecular Modelling* 92 (Proceedings of the 9th European Symposium on Structure-Activity Relationships: QSAR and Molecular Modelling), ESCOM, Leiden, 1993, pp. 52-58.
- 12 Pang, Y.-P. and Kozikowski, A.P., *J. Comput.-Aided Mol. Design*, 8 (1994) 669.
- 13 Kozikowski, A.P., Ma, D., Pang, Y.-P., Shum, P., Likic, V., Mishra, P.K., Macura, S., Basu, A., Lazo, J.S. and Ball, R.G., *J. Am. Chem. Soc.*, 115 (1993) 3957.
- 14 Bernstein, F.C., Koetzle, T.F., Williams, G.J., Meyer Jr., E., Brice, M.D., Rodgers, J.R., Kennard, O., Shimanouchi, T. and Tasumi, M., *J. Mol. Biol.*, 112 (1977) 535.
- 15 Villalobos, A., Blake, J.F., Biggers, C.K., Butler, T.W., Chapin, D.S., Chen, Y.P.L., Ives, J.L., Jones, S.B., Liston, D.R., Nagel, A.A., Nason, D.M., Nielsen, J.A., Shalaby, I.A. and White, W.F., *J. Med. Chem.*, 37 (1994) 2721.
- 16 Sugimoto, H., Tsuchiya, Y., Sugumi, H., Higurashi, K., Karibe, N., Iimura, Y., Sasaki, A., Araki, S., Yamanishi, Y. and Yamatsu, K., *J. Med. Chem.*, 35 (1992) 4542.
- 17 Burley, S.K. and Petsko, G.A., *Science*, 229 (1985) 23.
- 18 Hunter, C.A. and Sanders, K.M., *J. Am. Chem. Soc.*, 112 (1990) 5525.